Role for the epidermal growth factor receptor in neurofibromatosis-related peripheral nerve tumorigenesis

Benjamin C. Ling,[1,2,6] Jianqiang Wu,[1,6] Shyra J. Miller,[1] Kelly R. Monk,[1] Rania Shamekh,[1] Tilat A. Rizvi,[1] Gabrielle DeCourten-Myers,[3] Kristine S. Vogel,[4] Jeffrey E. DeClue,[5] and Nancy Ratner[1,*]

[1]Departments of Cell Biology, Neurobiology, and Anatomy
[2]Department of Neurosurgery
[3]Department of Pathology, University of Cincinnati College of Medicine, Cincinnati, Ohio 45267
[4]The Department of Cellular and Structural Biology, University of Texas Health Science Center at San Antonio, San Antonio, Texas 78229
[5]Laboratory of Cellular Oncology, National Cancer Institute, Bethesda, Maryland 20892
[6]These authors contributed equally to this work.
*Correspondence: nancy.ratner@cchmc.org

Summary

Benign neurofibromas and malignant peripheral nerve sheath tumors are serious complications of neurofibromatosis type 1. The epidermal growth factor receptor is not expressed by normal Schwann cells, yet is overexpressed in subpopulations of *Nf1* mutant Schwann cells. We evaluated the role of EGFR in Schwann cell tumorigenesis. Expression of EGFR in transgenic mouse Schwann cells elicited features of neurofibromas: Schwann cell hyperplasia, excess collagen, mast cell accumulation, and progressive dissociation of non-myelin-forming Schwann cells from axons. Mating EGFR transgenic mice to *Nf1* hemizygotes did not enhance this phenotype. Genetic reduction of EGFR in *Nf1*$^{+/-}$;*p53*$^{+/-}$ mice that develop sarcomas significantly improved survival. Thus, gain- and loss-of-function experiments support the relevance of EGFR to peripheral nerve tumor formation.

Introduction

Neurofibromatosis type 1 (NF1) is an autosomal dominant disorder, affecting approximately 1 in 3500 people (Huson, 1998; Riccardi, 1992) The hallmark of NF1 is the development of up to thousands of benign and slow-growing neurofibromas; more aggressive peripheral nerve tumors, known as malignant peripheral nerve sheath tumors (MPNSTs), develop in 5–10% of patients (Evans et al., 2002; Friedman and Birch, 1997). The *Nf1* gene on chromosome 17q11 encodes neurofibromin, a Ras-GAP (Wallace et al., 1991; Xu et al., 1990). Mutations in both *Nf1* alleles in some neurofibroma Schwann cells and in MPNSTs indicate that neurofibromin functions as a tumor suppressor (Legius et al., 1993; Sawada et al., 1996; Serra et al., 1997). Ras activation (Feldkamp et al., 1999; Sherman et al., 2000) and invasiveness of neurofibroma Schwann cells (Sheela et al., 1990) from human tumors support the idea that Schwann cells play a key role in neurofibroma formation.

Animal models of neurofibromatosis that accurately mimic the peripheral nerve manifestations of the disease were challenging to develop. In *Nf1* knockout mice, no peripheral nerve pathology exists in heterozygotes; offspring null at *Nf1* die in utero by E13 due to cardiac defects (Brannan et al., 1994; Gitler et al., 2003; Jacks et al., 1994). Targeted deletions at both alleles in chimeric mice (Cichowski et al., 1999; Vogel et al., 1999) and most recently with the use of a conditional cre/lox allele in Schwann cells in combination with a hemizygous *Nf1* deficient environment (Gitler et al., 2003; Zhu et al., 2002) produced peripheral nerve pathology with features similar to plexiform neurofibromas.

We have focused on identifying molecular alteration in cells and tumors associated with *Nf1* mutation in cultures and animal models. These studies have led to identification of aberrant expression of the epidermal growth factor receptor (EGFR; ErbB1) in these tumor cells, and an EGFR-inducible protein, BLBP, that may regulate Schwann cell-axon interaction in these models (DeClue et al., 2000; Li et al., 2002; Miller et al., 2003). Specifically, EGFR is expressed in primary MPNST, MPNST cell lines, and some S100+ Schwann cells in primary neurofibromas (DeClue et al., 2000). 23 of 24 cell lines derived from malignant soft tissue sarcomas from *Nf1:p53* compound heterozygous mice were also found to express EGFR (Li et al., 2002). EGFR gene amplification is also observed in MPNSTs (Perry et al., 2002). The identification of EGFR was of particular interest, as

SIGNIFICANCE

An ongoing debate in neurofibromatosis research is whether *Nf1* mutant Schwann cells need cooperation from mutant surrounding cells to drive neurofibroma formation. This paper shows that EGFR expression in Schwann cells not only produces a tumor-like phenotype in Schwann cells, but also drives mast cell accumulation and fibrosis typical of human neurofibromas, without a mutant environment. The work defines a model of early neurofibroma formation. In contrast to EGFR mutant brain tumor models, in the peripheral nerve, a wild-type *EGFR* allele drives tumorigenesis. This work supports possible clinical utility of EGFR antagonists in NF1.

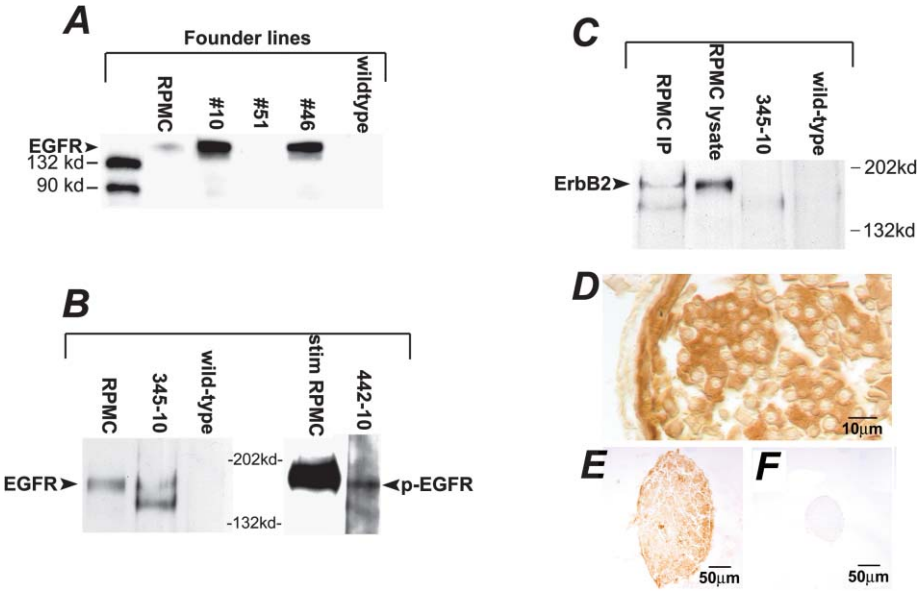

Figure 1. Human EGFR protein is expressed in CNPase-hEGFR transgenic mice

A: Western immunoblot of immunoprecipitates from brain lysates demonstrating protein expression of hEGFR in two transgenic founder lines. Positive control: RPMC cell line (human melanoma) known to express EGFR and ErbB2.

B: Sciatic nerve expression of hEGFR confirmed with specimen 345–10, and demonstration of active phosphorylated EGFR seen in spinal cord lysate of specimen 442–10, after immunoprecipitation. Positive control: RPMC cells stimulated with EGF.

C: Demonstration of lack of heterodimer formation between hEGFR and ErbB2: lysates were immunoprecipitated with anti-hEGFR and blots probed for ErbB2. No band noted in specimen 345–10, as compared to positive control RPMC cells, which do exhibit heterodimer formation.

D: Immunohistochemistry of saphenous nerve demonstrating cell-specific hEGFR expression with positive Schwann cell sheath staining and lack of axonal staining.

E and F: Low magnification saphenous nerve staining for hEGFR in transgenic specimen (**E**) is compared to lack of staining in wild-type specimen (**F**).

it is overexpressed or expressed as an active mutant in gliomas and in breast, endometrial, ovarian, colon, and cervical cancers (Yarden, 2001). Normal Schwann cells respond to products of the *neuregulin-1* gene, called neuregulins (Garratt et al., 2000; Levi et al., 1995; Morrissey et al., 1995). These are ligands for the receptor tyrosine kinases ErbB3 and ErbB4, which bear homology to EGFR (Prenzel et al., 2001). Wild-type Schwann cells express the non-ligand-binding kinase ErbB2 and ErbB3, but not EGFR (DeClue et al., 2000; Levi et al., 1995). Based on these studies, we hypothesized that Schwann cell expression of EGFR might be important in neurofibroma and/or MPNST development, and tested this idea by developing a transgenic mouse strain expressing wild-type EGFR under control of a Schwann cell promoter. We also show that genetic decrease of EGFR in a mouse model system of neurofibromatosis-related malignancy reduces tumorigenesis.

Results

hEGFR expression, dimerization, and activation in transgenic mice

To test the role of EGFR in neurofibroma formation, we developed transgenic mice in which the 2′3′-cyclic nucleotide 3′-phosphodiesterase (CNP) promoter, specific for Schwann cells in peripheral nerve (Chandross et al., 1999; Gravel et al., 1998; Tsukada and Kurihara, 1992; Weissbarth et al., 1981), drives expression of human EGFR. We raised and bred four founder mice, and confirmed presence of the hEGFR transgene in two lines, designated CNP-hEGFR #10 and #46. Transgene integration effects are unlikely, as two independent lines of mice demonstrated pathology described below. We confirmed hEGFR protein expression with monoclonal anti-human EGFR antibody to probe Western blots after immunoprecipitation with a polyclonal anti-EGFR antibody (Figure 1A). We detected robust hEGFR expression using the same method in brain and spinal cord, where CNP drives expression in oligodendrocytes, with only trace expression in non-nervous tissues (Figure 1A). We also detected hEGFR in sciatic nerve lysates from transgenic but not wild-type mice (Figure 1B, left).

Ligand binding to the EGFR causes receptor autophosphorylation, which leads to receptor activation as docking sites are created for signaling proteins (Prenzel et al., 2001). To test if expressed hEGFR in the transgenic mice is activated, we probed Western blots of sciatic nerve lysates precipitated with anti-human EGFR antibodies with an anti-phospho-EGFR antibody (Santa Cruz Biotech, Santa Cruz, California). Sciatic nerve lysates from CNP-hEGFR mice contained phosphorylated hEGFR (Figure 1B, right), while lysates from wild-type nerves did not (not shown). Consistent with a low level of phosphorylated EGFR, we found no detectable changes in Ras-GTP or AKT-phosphorylation in Schwann cells from the mutant nerves as compared to wild-type cells (data not shown).

Ligand binding to EGFR can induce homodimerization or heterodimerization with ErbB2 or ErbB4 (Murali et al., 1996; Prenzel et al., 2001). Receptor dimerization is necessary for receptor activation. Schwann cells do not express ErbB4. We tested if hEGFR/ErbB2 dimers are present in nerves from transgenic mice. HEGFR formed no detectable heterodimers with ErbB2 in nerve lysates, although we easily detected dimers in lysates from control RPMC cells (Figure 1C). Thus, hEGFR likely exists as homodimers in CNP-hEGFR nerve. EGFR depends on ligands for homodimerization and activation (Prenzel et al., 2001). It is known that hEGFR transfected into mouse cells signals appropriately when stimulated by ligand (Velu et al., 1987). We analyzed expression of EGFR ligands in wild-type and CNP-hEGFR sciatic nerves by quantitative real-time PCR (QRT-PCR). We detected betacellulin, HB-EGF, and TGF-α in wild-type and CNP-hEGFR nerves at approximately equivalent levels. No message was detected for EGF, epiregulin, or amphiregulin (Table 1). Schwann cells purified and expanded in culture expressed betacellulin and amphiregulin, confirming that pe-

Table 1. mRNAs encoding EGFR ligands are present in adult peripheral nerve and cultured Schwann cells

A: Ligands

	AR	BTC	EGF	EPIREG	HBEGF	TGF-α
WT nerve	−	+	−	−	+	+
EGFR nerve	−	+	−	−	+	+
MSC	−	+	−	−	−	+

B: Quantification of ligands present in nerve

BTC	BTC avg C_t	GAPDH avg C_t	ΔC_t	$\Delta\Delta C_t$	Fold change
W/T	31.94 ± 0.02	25.46 ± 0.49	6.48 ± 0.49	0.00 ± 0.49	1 (0.71–1.41)
EGFR	27.90 ± 0.02	27.76 ± 0.15	5.14 ± 0.15	−1.34 ± 0.15	2.53 (2.28–2.81)
HBEGF	HBEGF avg C_t	GAPDH avg C_t	ΔC_t	$\Delta\Delta C_t$	Fold change
W/T	31.42 ± 0.05	27.61 ± 0.50	3.81 ± 0.50	0.00 ± 0.60	1 (0.71–1.41)
EGFR	33.20 ± 0.23	30.35 ± 0.15	2.85 ± 0.27	−0.96 ± 0.27	1.94 (1.61–2.35)
TGF-α	TGF-α avg C_t	GAPDH avg C_t	ΔC_t	$\Delta\Delta C_t$	Fold change
W/T	29.00 ± 0.19	27.61 ± 0.50	1.39 ± 0.53	0.00 ± 0.53	1 (0.69–1.44)
EGFR	31.00 ± 0.23	30.35 ± 0.15	0.65 ± 0.27	−0.74 ± 0.27	1.67 (1.39–2.01)

A: Presence of EGFR ligand mRNA as detected by real-time PCR.
B: Quantification of ligands present in nerve. WT, wild-type; MSC, mouse Schwann cells; AR, amphiregulin; BTC, betacellulin; EGF, epidermal growth factor; EPREG, epiregulin; HBEGF, heparin-binding epidermal growth factor; TGF-α, transforming growth factor α.

ripheral glia make EGFR ligands (Table 1). The data are consistent with locally available ligands activating hEGFR receptors.

The CNP promoter drives expression in Schwann cells in peripheral nerve and oligodendrocytes in the central nervous system (Gravel et al., 1998). We stained sections of mouse nervous system for hEGFR using a species-specific anti-human EGFR antibody. We detected no obvious defects in brain oligodendrocytes, possibly due to unavailability of EGFR ligands in the brain. There may also be little effect of isolated EGFR signaling in oligodendrocytes even if ligands are available. In saphenous nerve, we detected labeling of myelinating Schwann cell sheaths and inter-axon endoneurium staining suggestive of nonmyelinating Schwann cells (NMSC); perineurium was not labeled (Figure 1D). We found no staining of wild-type nerve (Figure 1F) as compared to the much larger hEGFR saphenous nerve (Figure 1E). Levels of EGFR expression in Schwann cell lysates were similar to, or less than, those in 3 *Nf1;p53* cell lines that express EGFR by Western blotting (data not shown).

Nerves of CNPase-EGFR mice are enlarged

Neurofibromas enlarge nerves in NF1 patients. Gross inspection of intercostal nerves, sciatic nerves, cauda equina, and cutaneous nerve twigs indicated diffuse hypertrophy in all CNPase-hEGFR transgenic mice (data not shown). We gathered quantitative data on nerve size in saphenous nerve. Saphenous nerves are easily accessible in dissections and maintain a constant diameter, without branches, over a lengthy segment. We measured nerve cross-sectional area (Figure 2A). We noted a significant, up to 8-fold, increase in area of transgenic nerves in comparison to wild-type nerves ($p = 0.001$). Hypertrophy was also noted in cranial nerves of transgenic mice (data not shown).

Hypercellularity in CNPase-hEGFR nerves

The histological basis of the nerve hypertrophy in CNPase-hEGFR mice is attributable at least in part to hypercellularity. We counted nuclei in hematoxylin-stained nerve cross-sections and found them to beincreased 2- to 8-fold in hEGFR nerves ($p = 0.01$, Figure 2B). In contrast, there was no significant change in number of myelinated axons: wild-type saphenous nerves

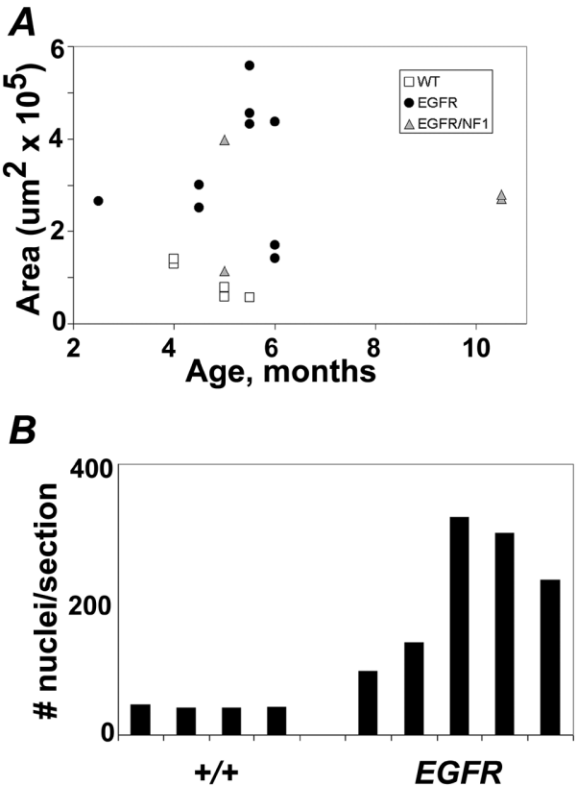

Figure 2. CNPase-hEGFR nerves are enlarged and hypercellular

A: Cross-sectional area of saphenous nerves plotted with respect to age and distinguished by genotype. Significant enlargement of CNPase-hEGFR and CNPase-hEGFR, $Nf1^{+/-}$ nerves compared to wild-type ($p = 0.001$ and $p = 0.008$, respectively) is seen.
B: Nuclei counts from saphenous nerve cross-sections accomplished by hematoxylin staining. CNPase-hEGFR nerves have significantly increased nuclei ($p = 0.01$).

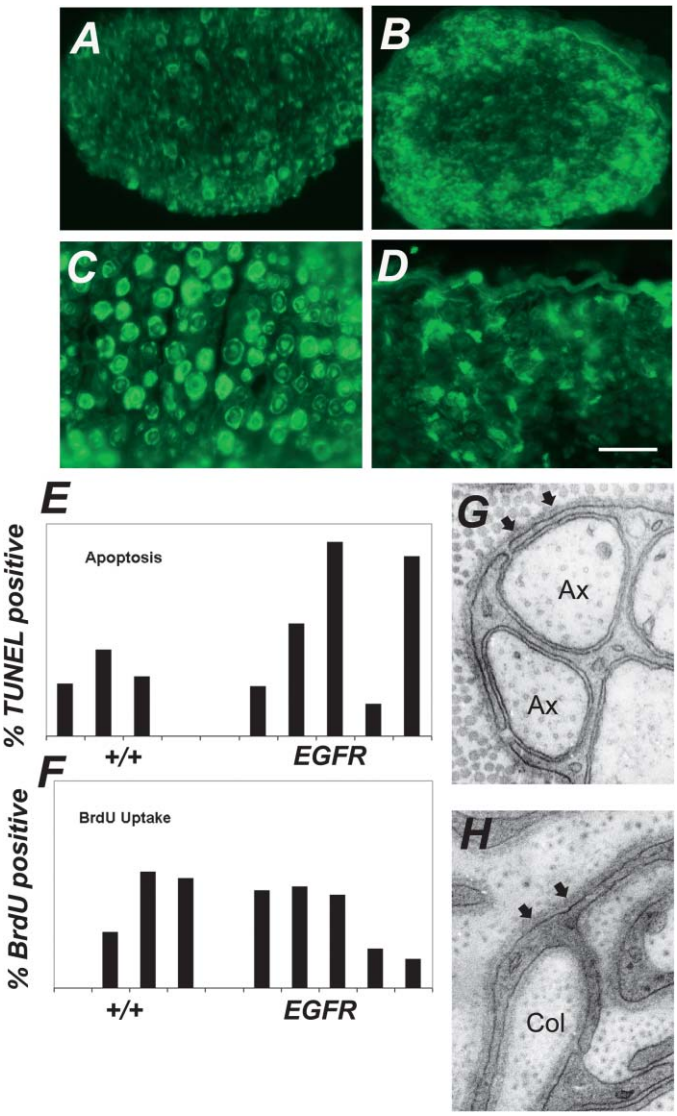

Figure 3. Hypercellularity is attributable to Schwann cells

A–D: Markers for Schwann cells: S100 staining of saphenous nerve cross-sections in wild-type (**A**) and CNPase-hEGFR (**C**) mice, and p75 staining in wild-type (**B**) and CNPase-hEGFR (CM #69) (**D**) mice.

E and F: Assessment of apoptosis rates by TUNEL staining (**E**) and BrdU uptake (**F**) over 6 hr in saphenous nerve cross-sections showing no significant difference between wild-type and CNPase-hEGFR nerves.

G and H: Electron micrographs: presence of a basal lamina (small arrows) around a nonmyelinating Schwann cell and its ensheathed axons (Ax) in wild-type nerve (**G**). Basal lamina is present around membrane processes in a CNPase-hEGFR nerve (**H**), indicating Schwann cell origin.

harbored on average 465 large axons, while transgenic nerves averaged 499 (n = 3 each; p = 0.32). Increased numbers of endoneurial cells in mutant nerves could result from increased proliferation and/or decreased cell death. We analyzed entry into S phase of endoneurial cells in mutant nerves by labeling with BrdU. In wild-type adult nerves, we detected the expected low proliferation rate (0.4%) in 6 hr as previously reported (Brown and Asbury, 1981). While the absolute numbers of BrdU-positive nuclei were higher in transgenic nerves, the ratio of positive nuclei to total nuclei was not significantly different (p = 0.96) (Figure 3F). We analyzed cell death as measured by TUNEL-positive nuclei. We found 0.4% TUNEL-positive nuclei in wild-type nerves (Grinspan et al., 1996); numbers of positive nuclei in transgenic mice were not significantly different (p = 0.16, Figure 3E). Thus, ongoing increases in cell proliferation or decreased cell death are not detectable in adult nerves. Cell number increases may therefore occur at low levels throughout the life of the animal, and/or at earlier times (see below). Human neurofibroma cells also show little proliferation and death (Kourea et al., 1999).

Hyperplastic endoneurial cells in transgenic nerves might be Schwann cells, fibroblasts, and/or perineurial cells; each is present at variable levels in neurofibromas. Wild-type and CNPase-hEGFR nerve cells associated with myelin sheaths showed cytoplasmic S100-positive staining, as expected for myelinating Schwann cells (Mata et al., 1990) (Figures 3A and 3C), and p75NGFR immunoreactivity characteristic of non-myelin-forming Schwann cells (NMSCs) (Figures 3B and 3D). Greater than 90% of nuclei unassociated with myelin sheaths were surrounded by GFAP-positive cytoplasm, supporting a NMSC phenotype (Jessen et al., 1990). Continuous basal lamina characteristic of Schwann cells were present on >90% of cells in the endoneurium of CNPase-hEGFR saphenous nerves in electron micrographs (Figures 3G and 3H). Most endoneurial cells are therefore Schwann cells; others may be fibroblasts or perineurial cells.

Unmyelinated fiber bundles and nonmyelinating Schwann cells in CNPase-hEGFR mice exhibit marked alterations which worsen with time

We analyzed electron micrographs to define nerve pathology. Normal 4-month-old saphenous nerve contains large axons surrounded by single myelin-forming Schwann cells and groups of smaller axons ensheathed together by individual NMSCs (Figure 4B). The same age transgenic saphenous nerves were abnormal (n = 5) (Figures 4A, 4D, and 4E). NMSCs displayed long aberrant processes which wrapped one or two, or no, small axons. Collagen fibers filled the nerve matrix between large myelinated axons and were frequently, errantly, "wrapped" by Schwann cell processes (Figures 3H and 4E, inset). Notably, many Schwann cells in neurofibromas lack contact with axons.

The increased size of CNPase-hEGFR nerves results from an increase in the number of nerve Schwann cells (Figure 2B), increased collagen, and increased myelin thickness. We measured myelin sheath thickness (n = 100) and the distance between myelin sheaths (n = 100) in electron micrographs from 3 wild-type and 3 CNPase-hEGFR saphenous nerves. Both parameters were increased (p < .0001; Wilcoxon nonparametric test).

We observed the nerve pathology worsen with time. We examined saphenous nerves at 4 months of age (n = 2) and found that nerves had NMSCs with aberrant processes. Our cohort studied by EM included 2-month-old (n = 2), 4-month-old (n = 5), and 6-month-old (n = 2) transgenic mice. Nerves progressively accumulated collagen and dysfunctional Schwann cells, and had increasing numbers of disrupted small axonal fiber bundles (Figures 4F–4H). These patterns of pathology suggest a degenerative neuropathy of small caliber axons.

CNPase-hEGFR nerves exhibit increased mast cell infiltration and fibrosis

Neurofibromas contain more mast cells than normal nerve (Johnson et al., 1990). We observed granule-laden mast cells in

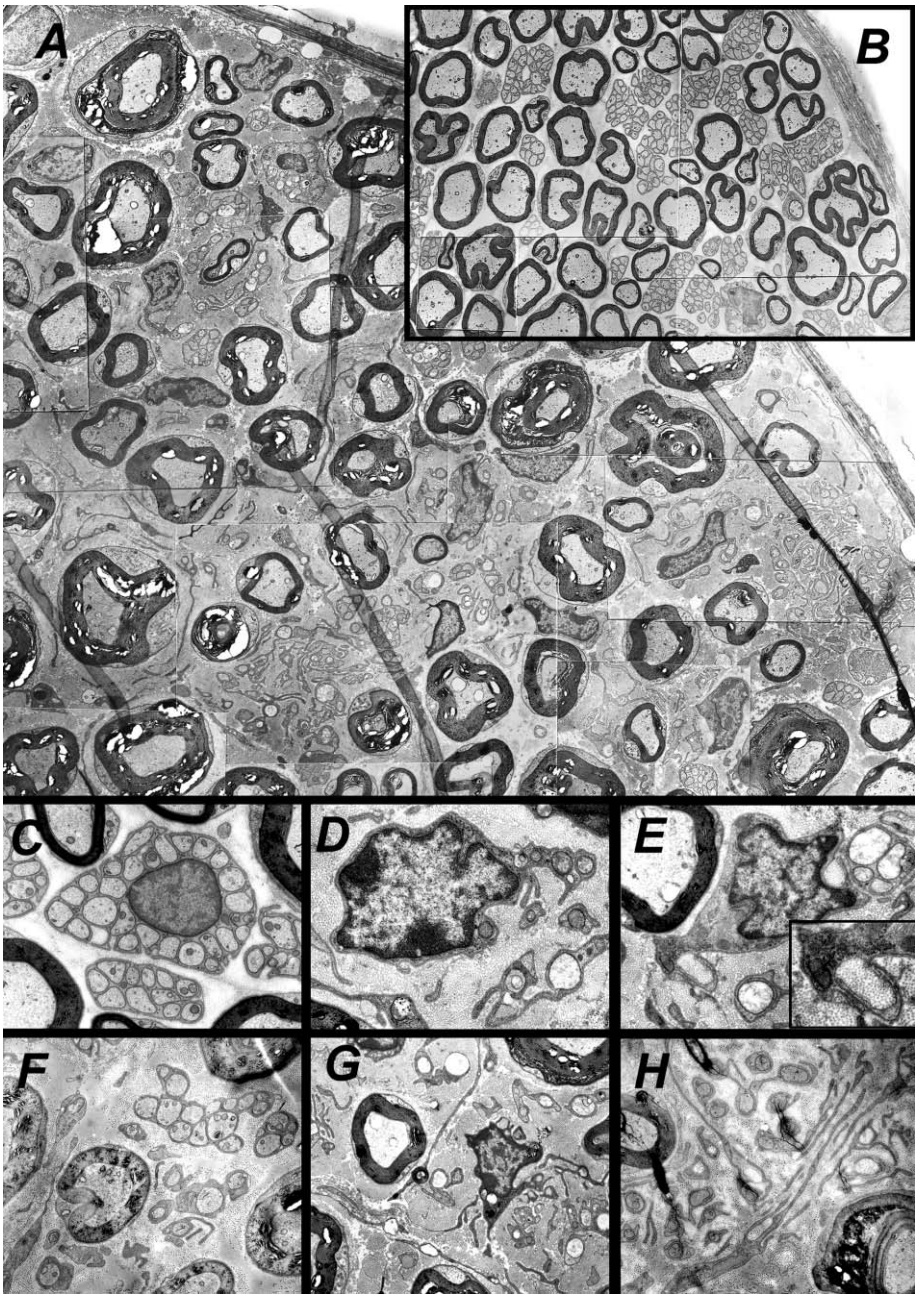

Figure 4. Ultrastructural studies show pathology of CNPase-hEGFR nerves

A: Electron micrograph montage of CNPase-hEGFR saphenous nerve.
B: In comparison, wild-type saphenous nerve at the same magnification.
C: A normal nonmyelinating Schwann cell nucleus with cell membrane wrapping of small axons in wild-type nerve.
D–H: A markedly dysmorphic nucleus in CNPase-hEGFR nerve with membrane wrapping of a limited number of axons (**D**), and another example (**E**) showing Schwann cell processes with no association with any axons and pathologic wrapping of collagen fibrils (inset). Pathology is seen to progress with time in CNPase-hEGFR nerves comparing a 2.5-month-old specimen (**F**) to a 4-month-old specimen (**G**) and to a 6-month-old specimen (**H**).

electron micrographs of hEGFR nerves (Figure 5A) and toluidine blue-stained saphenous cross-section (Figure 5B). We counted mast cells in saphenous nerve cross-sections. Mast cell numbers were significantly increased in adult transgenic mouse nerves compared to the wild-type counterpart ($p = 0.004$) (Figure 5C). Many mast cells were degranulating. Mast cell chemoattractants BDNF, MCP-1, SCF, TGF-β1, and VEGF were each upregulated in mutant nerves as determined by QRT-PCR (Figure 5D), likely accounting for the additional mast cells. Schwann cell hyperplasia precedes mast cell accumulation. Compared to the adult mice, in 4-week-old mice, Schwann cell numbers increased significantly in EGFR nerves (Figure 5E), while mast cell numbers did not (Figure 5F). As mast cell products induce fibrosis, we confirmed enhanced collagen deposition by trichrome stain (Figures 5G and 5H).

CNPase-hEGFR;*Nf1*$^{+/-}$ mice do not show evidence of worsening pathology

Loss-of-function of *Nf1* in Schwann cells cooperates with *Nf1*$^{+/-}$ in other cells in one NF1 mouse model (Zhu et al., 2002). To examine if *Nf1*$^{+/-}$ worsened the CNPase-hEGFR nerve phenotype, we bred CNPase-hEGFR mice with *Nf1*$^{+/-}$ mice. Dissection along the neuroaxis and peripheral nervous system of double heterozygous mice revealed similar diffuse nerve enlargement as in CNPase-hEGFR mice. Saphenous nerves of 4 double-heterozygous mice were significantly larger ($p = 0.0075$)

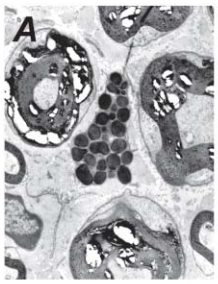

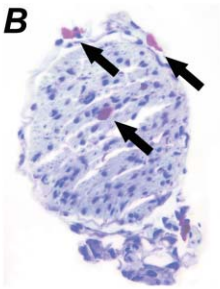

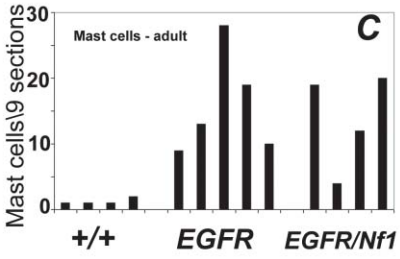

D Chemoattractant	Expression: Not Detected +/+ or EGFR nerve	Similar levels +/+ and EGFR nerve	Fold change +/+ to EGFR nerve
Anaphylatoxin C3a	+		
Anaphylatoxin C5a	+		
BDNF			↑*
Eotaxin	+		
Fractalkine	+		
IL-6		+	
LIF	+		
MCP-1			↑*
NGF		+	
Neurotrophin-3	+		
Rantes		+	
PAR			
Serum amyloid A	+		
SCF			+2.45 (2.06-2.91)
TGF-β1			↑*
VEGF			+2.65 (+2.21—3.18)

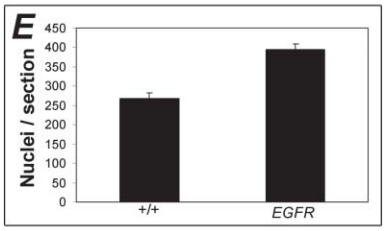

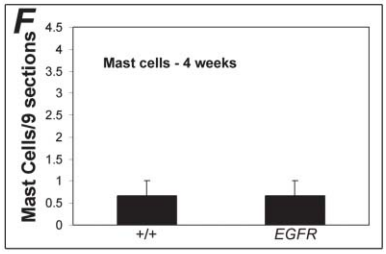

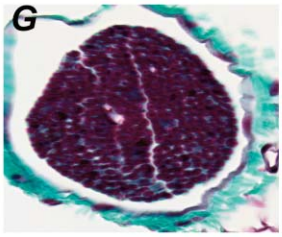

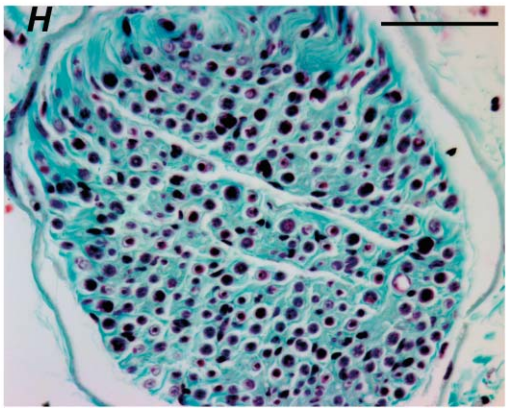

Figure 5. Mast cells and fibrosis in CNPase-hEGFR mouse nerves

A: Mast cell seen in CNPase-hEGFR saphenous nerve on electron micrograph.
B: Toluidine blue staining of CNPase-hEGFR saphenous nerve cross-section showing multiple metachromatic mast cells (arrows).
C: Mast cell counts in saphenous nerves, comparing wild-type mice (+/+) to CNPase-hEGFR mice (EG) to CNPase-hEGFR;*Nf1*$^{+/-}$ mice (EG/NF). CNPase-hEGFR and CNPase-hEGFR;*Nf1*$^{+/-}$ nerves harbor significantly more mast cells ($p = 0.004$ and $p = 0.015$, respectively) than wild-type nerves.
D: Differential expression of mast cell chemoattractants mRNA in adult hEGFR or wild-type mouse nerves as detected by real-time PCR. *, expressed only in hEGFR nerve.
E: Total nuclei are increased in 4-week-old mouse sciatic hEGFR nerves ($p < 0.0001$).
F: Mast cell counting from toluidine blue stained 4 weeks old mice saphenous nerve cross-sections.
G and H: Wild-type saphenous nerve cross-section stained with Gamori's trichrome (**G**) showing relative paucity of collagen (green) as compared to CNPase-hEGFR nerves at 6 months (**H**). Bar in **G** and **H** = 500 μM.

compared to wild-type mice, but not significantly different ($p = 0.41$) from nerves of mice which were only EGFR-positive (Figure 2A; triangles).

CNPase-hEGFR mice develop rare nerve tumors

We aged 19 CNPase-hEGFR and 12 wild-type littermates until moribund. 42% of EGFR mice and 50% of wild-type mice remained alive at 23 months. We observed nerve thickening in 11 EGFR mice evaluated at autopsy, but found no consistent cause of death. We observed a grossly enlarged spinal nerve root in one mouse diagnosed as a neurofibroma (Figure 6A). Another mouse developed a nerve-associated spindle cell tumor with muscle differentiation (Figure 6B). Desmin and S100 staining (Figures 6C and 6D) were positive, confirming a diagnosis of triton tumor. We used an anti-human EGFR antibody to probe Western blots after immunoprecipitation of brain and tumor lysates from this mouse with a polyclonal anti-EGFR antibody (Figure 6E). hEGFR was enriched in the tumor, demonstrating transgene association. We analyzed six CNPase-EGFR/*Nf1*$^{+/-}$ mice. Nerve thickening was consistent, but no nerve tumors were detected, and no consistent cause of death was found. These data suggest that EGFR expression can lead to peripheral nerve tumorigenesis, benign and malignant, but that frank tumor formation in this model is rare, even when mice are hemizygous for *Nf1* mutation.

Diminshed EGFR signaling decreases mortality in the *Nf1;p53* mouse tumor model

To determine whether EGFR expression is important for *Nf1*-associated tumor formation, we mated *Nf1*$^{+/-}$;*p53*$^{+/-}$mice to EGFR$^{wa\text{-}2}$/+ mice. As previously described, *Nf1*$^{+/-}$;*p53*$^{+/-}$ mice develop sarcomas and brain tumors at as early as 15 weeks of

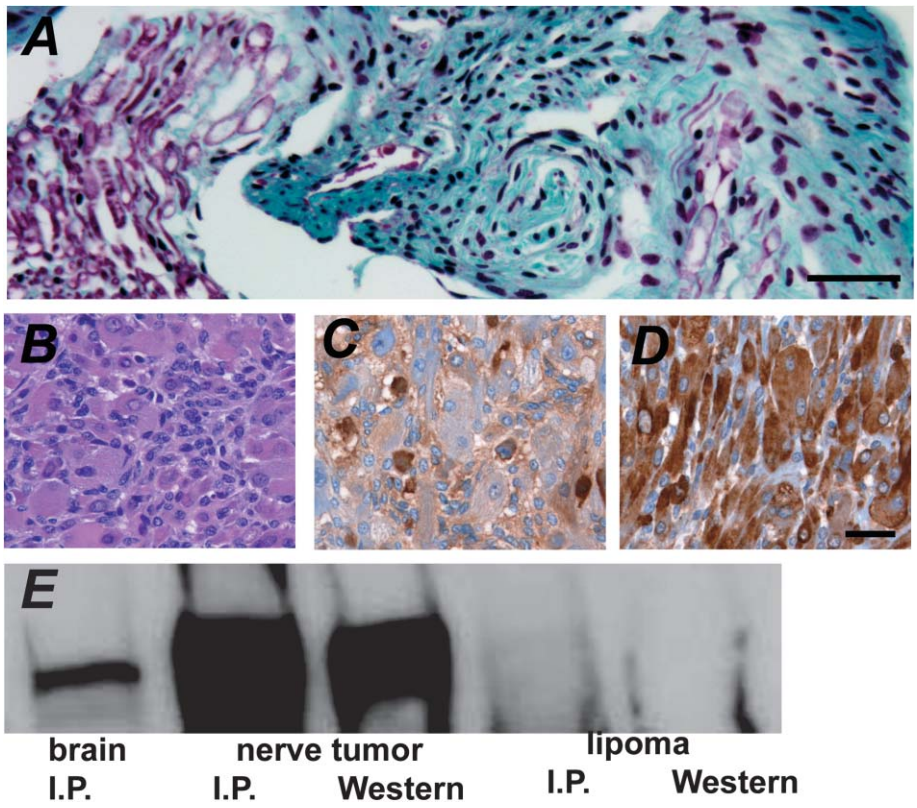

Figure 6. Tumors of CNPase-hEGFR mouse nerves

A: Enlarged spinal nerve root, diagnosed as a neurofibroma, from CNPase-hEGFR mouse.
B–D: Rhabdomyosarcoma from CNPase-hEGFR mouse (H&E). This was confirmed with S100 (**C**) and desmin (CM #69) (**D**) staining.
E: Western immunoblot of immunoprecipitates of brain and rhabdomyosarcoma lysates from this mouse, demonstrating enriched hEGFR expression in the tumor. No expression of hEGFR was seen in a lipoma from the same mouse.
Scale bar in A–D = 1000 μM.

age (Cichowski et al., 1999; Vogel et al., 1999; Reilly et al., 2000). EGFR$^{Wa\text{-}2}$/+ mice contain a point mutation in EGFR that reduces receptor tyrosine kinase activity by >90%. *Nf1*$^{+/-}$;*p53*$^{+/-}$ and *Nf1*$^{+/-}$;*p53*$^{+/-}$;EGFR$^{wa\text{-}2}$/+ littermates were followed for six months. We compared mortality of the *Nf1*$^{+/-}$;*p53*$^{+/-}$ mice (n = 19) with the *Nf1*$^{+/-}$;*p53*$^{+/-}$;EGFR$^{wa\text{-}2}$/+ mice (n = 17) (Figure 7). Strikingly, reduced EGFR activity decreased tumor formation time and mortality significantly ($p < 0.05$). In this study, 11 of 19 *Nf1*$^{+/-}$;*p53*$^{+/-}$ mice (57.9%) developed malignant tumors and died by 26 weeks. In contrast, only 1 of 17 (5.9%) *Nf1*$^{+/-}$;*p53*$^{+/-}$;EGFR$^{wa\text{-}2}$/+ was dead at this time. This mouse required sacrifice at 21 weeks due to a large periorbital mass, pathologically diagnosed as a spindle cell tumor. Focal S100 immunoreactivity and some mitotic activity allowed diagnosis of a GEM PNST, grade II (Stemmer-Rachamimov et al., 2004). The remaining 16 mice remain healthy. Thus, decreased levels of EGFR delay tumor formation and mortality in the *Nf1*$^{+/-}$;*p53*$^{+/-}$ model.

Discussion

This study demonstrates the dramatic effect of expressing EGFR in mouse Schwann cells. Peripheral and cranial nerves in CNP-hEGFR mice exhibit diffuse changes that parallel the hallmarks of human cutaneous and plexiform neurofibromas. These include increased endoneurial collagen matrix, dissociation of Schwann cells from axons, Schwann cell hypercellularity, and mast cell accumulation. Changes were within the perineurium, as is common in plexiform neurofibromas. While previous studies showed that EGFR is expressed in MPNST cells and some neurofibroma Schwann cells (DeClue et al., 2000; Li et al., 2002), EGFR expression might have correlated with tumor formation, rather than being a causative event. Strikingly, our data are consistent with a causative, and early, role for EGFR in progression to neurofibroma formation. EGFR overexpression

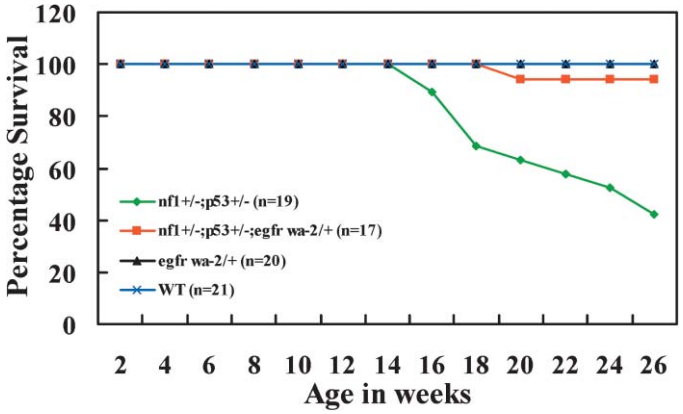

Figure 7. Improved survival of *Nf1*$^{+/-}$;*p53*$^{+/-}$;Egfr^{wa2}/+ mice

Mice were housed in a temperature- and humidity-controlled pathogen-free viaticum and observed daily for evidence of illness or tumor formation. Mice were sacrificed if palpable tumor exceeded 1 cm in diameter or interfered with feeding and grooming. Green, *Nf1*$^{+/-}$;*p53*$^{+/-}$ (n = 19); red, *Nf1*$^{+/-}$;*p53*$^{+/-}$;Egfr^{wa2}/+ (n = 17); black, Egfr$^{wa\text{-}2}$/+ (n = 20); and blue, wild-type (WT) (n = 21). The six-month survival of *Nf1*$^{+/}$;*p53*$^{+/-}$;Egfr^{wa2}/+ mice was significantly different from *Nf1*$^{+/-}$;*p53*$^{+/-}$ mice in a Kaplan-Meier survival analysis using SPSS software (p = .038).

is characteristic of, and contributes to, formation of many other human cancers. Therapeutic reagents that target EGFR are in clinical trials (Cunningham et al., 2004; Noble et al., 2004; Ranson et al., 2002; Yarden, 2001), and, based on our data, could be considered as candidate therapeutics for NF1.

EGFR is not normally expressed in peripheral nerve Schwann cells. We used the CNP promoter to drive hEGFR expression in Schwann cells and specifically localized hEGFR to glial cells in endoneurium. It was possible that hEGFR heterodimerization with Schwann cell-expressed ErbB2 might occur, but we failed to detect such heterodimers in adult nerves. We demonstrated EGFR ligand expression in peripheral nerve, and in wild-type Schwann cells. Based on these findings, it is likely that hEGFR expressed in Schwann cells homodimerize upon ligand stimulation, and become activated. Indeed, we detected phosphorylation of hEGFR in nerves.

This new model provided the opportunity to study early stages in neurofibroma formation, as pathology worsened with age and proximally to distally. Electron microscopy showed that abnormal axon-glial interactions were present by 2 months of age. Schwann cells wrapped progressively fewer axons, and ultimately dissociated from axons and wrapped collagen fibrils. Effects of hEGFR expression were significantly greater on nonmyelinating Schwann cells than on those associated with myelin, even though both Schwann cell types expressed hEGFR. This is consistent with enhanced sensitivity of the nonmyelinating Schwann cell to perturbed tyrosine kinase signaling downstream of hEGFR, driving abnormal neuron-glial interactions. Emphasizing a role for critical levels of tyrosine signaling in axon-glial interactions, Chen et al. (2003) showed that expression of a dominant negative ErbB4 receptor signaling in adult nonmyelinating Schwann cells causes progressive sensory loss with disruption of nonmyelinating Schwann cell bundles. Loss of the adhesion molecule L1 might also be involved, as mice without L1 also show disrupted nonmyelinating axon-Schwann cell units (Haney et al., 1999). Human neurofibromas preferentially arise from sensory nerves that contain mainly unmyelinated Schwann cells. Based on our results, many neurofibroma Schwann cells free of axons may have been associated at one time with small axons.

Mast cell accumulation and fibrosis are characteristic features of human neurofibromas and of peripheral nerves in hEGFR mice. Mast cells did not express hEGFR on Western blotting or immunostaining of tissue sections (data not shown). Perineurial cells, of mesodermal origin, were also negative for transgene expression. Nonglial cells accounted for few of the cells in the hEGFR nerves. It is reasonable to postulate that hEGFR signaling in Schwann cells stimulates production and secretion of mast cell chemoattractants, and here we have confirmed that mRNA encoding the mast cell chemoattractants BNDF, MCP-1, SCF, TGFβ1, and VEGF are each upregulated in mutant nerve; one or more may recruit mast cells to the nerve. Mast cells migrate to SCF secreted by Schwann cells (Yang et al., 2003). Mast cell degranulation stimulates collagen deposition by fibroblasts. Fibrosis is commonly linked to mast cell degranulation (Krishnaswamy et al., 2001). Thus, Schwann cell hEGFR expression could promote multicellular changes in peripheral nerve.

It remains possible that Schwann cell overexpression of tyrosine kinase receptors in addition to EGFR could drive the Schwann cell hyperplasia with fibrosis and mast cell accumulation documented. To our knowledge, to date, no other studies have examined transgenic overexpression of tyrosine kinase receptors in Schwann cells. However, the specificity of our result is suggested, in that Schwann cell transgenic overexpression of GGFβ3, a ligand for ErbB3, results in peripheral neuropathy, but not in the fibrosis and mast cell accumulation that we report (Huijbregts et al., 2003). Prenatal treatment of mice with the chemical carcinogen ENU (N-nitrosoethylurea) causes activation of the ErbB2 tyrosine kinase in mouse Schwann cells (Buzard et al., 1999). Such exposure induces invasive Schwann cell tumors with interdigitating Schwann cell processes, cyst formation, and parallel arrays of elongated neoplastic Schwann cells in about 4% of mice from sensitive strains (Wechsler et al., 1979); C57Bl/6 mice, such as those in our study, are highly resistant. Carcinogen-induced mouse nerve tumors and growth factor overexpression result in nerve pathologies very different from those in the EGFR transgenic mice. Together with our study, these data strongly support a key role for tyrosine kinase pathways in regulation of non-myelin-forming Schwann cells in peripheral nerve.

To better understand the relevance of EGFR expression to malignant tumor formation, we mated *Nf1*$^{+/-}$;*p*53$^{+/-}$ mice to EGFR$^{wa\text{-}2}$/+ mice. In a mouse model of colon cancer, the wa-2 mouse decreased adenoma number and prolonged survival (Roberts et al., 2002; Sibilia et al., 2000). In this study, reduction in EGFR expression in *Nf1*$^{+/-}$;*p*53$^{+/-}$;EGFR$^{wa\text{-}2}$/+ mice decreased tumor formation and mortality significantly. This data supports a crucial role for EGFR downstream of *Nf*1 signaling. MPNST formation is rare in the CNPase-EGFR-expressing mice (shown here), as it is after chemical carcinogen exposure, affecting only 0.05% of sensitive mice (Wechsler et al., 1979). It is likely that additional genetic events are necessary for frequent malignancy in the CNPase-hEGFR model. Other tyrosine kinases are expressed in human MPNST (Badache et al., 1998) and could contribute to tumor growth. In human, EGFR is amplified in 26% of MPNST (Perry et al., 2002), so this receptor is likely to be relevant to human MPNST tumor formation as it is in the *Nf1*-driven tumor model studied here.

This study shows that EGFR expression in Schwann cells results in nerve hyperplasia with occasional neurofibroma formation. To develop neurofibromas at a higher rate, or malignancies, it may be necessary to cross these mice to strains with other mutations. Cre/lox mediated ablation of *Nf1* in Schwann cells resulted in nerve pathology similar to that observed here, but only when the mice were also hemizygous for *Nf1* mutation (Zhu et al., 2002). Our model does not require mast cells and/or fibroblasts to be *Nf1*$^{+/-}$, as crossing hEGFR to *Nf1*$^{+/-}$ mice did not increase nerve size or Schwann cell number. The similar phenotype of hEGFR nerves to nerves in mice and humans, with loss of function mutation at *Nf1* (Cichowski et al., 1999; Vogel et al., 1999; Zhu et al., 2002), suggests that when loss of *Nf1* predisposes Schwann cells, or their progenitors, to upregulate EGFR, neurofibroma formation ensues. This new model will allow testing of EGFR antagonists in vivo for their ability to prevent the formation of tumorgenic phenotypes. This study further validates EGFR as a potential target for therapeutic intervention in NF1 patients.

Experimental procedures

Generation of CNPase-hEGFR transgenic mice

We subcloned the 2′3′-cyclic nucleotide 3′-phosphodiesterase (CNP) promoter (Chandross et al., 1999) into a Bluescript (Stratagene, La Jolla, CA)

backbone. We inserted the human EGFR cDNA (Velu et al., 1987) into SstII and XhoI sites in the newly created multiple cloning site downstream of the promoter. We confirmed sequence integrity by DNA sequencing (UC sequencing core facility). We excised the promoter, EGFR cDNA, and SV40 polyadenylation signal with VspI and MluI, and injected it into C57BL/6-SJL hybrid mouse oocytes.

hEGFR localization

We prepared tissue extracts using 10 μl buffer (1% triton X100, 50 mM Tris [pH 7.4], 150 mM NaCl, 1 μg/ml aprotinin, 1 μg/ ml leupeptin, 1 μg/ml pepstatin, 1 mM PMSF)/mg tissue. We incubated lysates at 4°C overnight with goat polyclonal anti-EGFR (Santa Cruz sc-03g; Santa Cruz, CA), and then with protein A/G agarose beads (Santa Cruz). We subjected samples to SDS-PAGE on 4%–20% gradient gels, and probed blots with human specific mouse monoclonal anti-EGFR (Zymed; South San Francisco, CA) or with anti-phosphorylated EGFR (Santa Cruz). We developed blots using an enhanced chemiluminescence kit (Amersham/Pharmacia; Piscataway, NJ).

We studied EGFR dimer formation by immunoprecipitation using a human-specific mouse monoclonal anti-EGFR (Upstate Biotech #05-101, Lake Placid, NY). We ran 8% SDS-PAGE gels and probed blots with anti-ErbB2 (Oncogene Research c-neu; Cambridge, MA) or anti-hEGFR (Zymed). We used the RPM-MC human melanoma cell line known to express ErbB2 and EGFR as a positive control.

Immunohistochemistry and histology

We sacrificed mice by perfusion fixation with 4% paraformaldehyde and harvested sciatic and saphenous nerves. We embedded nerves in paraffin and cut 6 μm thick cross-sections; every fifth section was mounted to avoid double counting. We analyzed sciatic nerve sections proximal to the sciatic bifurcation. We stained sections with hematoxylin for nuclear counts, toluidine blue for mast cells, and Gamori's trichrome for collagen.

We stained paraffin sections using a human-specific mouse monoclonal anti-EGFR (Zymed). Sections were first blocked for one hour using the Zymed Histomouse kit. We used rabbit polyclonal anti-cow S100 (Dako, Carpenteria, CA) and anti p75 (Chemicon, Teincula, CA). For fluorescence microscopy, we used Alexa-488 fluorescent conjugated anti-rabbit secondary and counterstained with bisbenzamide (DAPI) to identify nuclei.

Schwann cell proliferation and apoptosis

We gave mice three intraperitoneal BrdU injections (0.05 mg/gm) at 2 hr intervals. We sacrificed mice, harvested nerves, and cut paraffin sections. We detected BrdU uptake with biotinylated anti-BrdU antibody (Zymed) followed by incubation with streptavidin-conjugated rhodamine (Jackson ImmunoResearch Corp; West Grove, PA). To quantify cell death, we used the TdT-FragEL DNA Fragmentation Detection Kit (Oncogene Research Products). We counted nuclei with DAPI costaining.

Examination of nerve ultrastructure

We perfusion-fixed anaesthetized mice with 3.2% glutaraldehyde with 3% paraformaldehyde in 0.1M cacodylate buffer for 10 min, followed by postfixation in situ for 20 min. We harvested sciatic and saphenous nerves, rinsed them with 0.1 M phosphate buffer, postfixed with 2% osmium tetroxide and 0.6% potassium ferrocyanide, and embedded them in Embed plastic. We stained semithin sections (1 μM) with toluidine blue to count myelinated axons by light microscopy. We viewed thin sections stained with uranyl acetate and lead citrate on a Jeol 100CX electron microscope.

Detection of EGFR ligands by quantitative real-time PCR

We extracted messenger RNA from wild-type and CNPase-hEGFR mouse sciatic nerves, or from mouse Schwann cells isolated as described (Kim et al., 1995), using the Micro-FastTrack kit (Invitrogen; Carlsbad, CA). We reverse transcribed mRNA using the Superscript Preamplification System (GibcoBRL; Grand Island, NY) with Superscript II reverse transcriptase, oligo-dT primers, and random hexamers per manufacturer's protocol. We controlled for genomic DNA contamination by omitting reverse transcriptase. We amplified GAPDH as a control (sense, 5′-ACCCAGAAGACTGTGGATGG-3′ and antisense, 5′- GGAGACAACCTGGTCCTCAG-3′; product size, 300 bp) for each sample. We carried out quantitative real-time PCR experiments in the presence of SYBR green using the primers amphiregulin (AR; sense, 5′-TGGCAGTGAACTCTCCACAG-3′ and antisense, 5′-CAATTGCATGTCA CCACCTC-3′; product size, 300 bp), betacellulin (BTC; sense, 5′-GGAACC TGAGGACTCATCCA-3′ and antisense, 5′-TCTAGGGGTGGTACCTGTGC-3′; product size, 227 bp), epidermal growth factor (EGF; sense, 5′-GAGAGG TGCAGAAGGACCTG-3′ and antisense, 5′-CACCAATTGCTGGTGATTTG-3′; product size, 271 bp), epiregulin (EPREG; sense, 5′-TTCAGATGGAA GACGATCCC-3′ and antisense, 5′-CGCAACGTATTCTTTGCTCA-3′; product size, 206 bp), heparin binding EGF (HBEGF; sense, 5′-ATAGCTTTGCGC TGTGACCT-3′ and antisense, 5′-CACACTCTTTGGTCCCACCT-3′; product size, 166 bp), and transforming growth factor-β (TGFβ; sense, 5′-TGTGTGA TAAAGCTGCCTGC-3′ and antisense, 5′-CAACCCTTTGAGGTTCGTGT-3′; product size, 100 bp). Cytokine primers are available on request. We preformed replicate reactions in an ABI Prism 7700 Sequence Detection System Cycler according to manufacturer's instructions. We confirmed all PCR products on 2% agarose gels. We calculated ΔC_t values relative to GAPDH expression. We calculated the fold changes in CNP-hEGFR nerves compared to wild-type nerves using the equation $2^{-\Delta\Delta Ct}$, where C_t is the cycle number at the chosen amplification threshold as determined by PE Biosystems software, $\Delta C_t = C_{t(ligand)} - C_{t(GAPDH)}$, and $\Delta\Delta C_t = \Delta C_{t(+/-)} - \Delta C_{t(+/+)}$ (K. Luvak, PE ABI Sequence Detector User Bulletin 2).

Mice and genotyping

Nf1$^{+/-}$;*p53*$^{+/-}$ mice carry the *Nf1* and *p53* mutations in *cis* on mouse chromosome 11 (Vogel et al., 1999). Mice had been backcrossed six generations onto the C57Bl/6 background at the time of the experiment. The tumor spectrum on this background has been described (Reilly et al., 2000). We obtained B6EiC3H-*Egfr*^{wa2} mice from the Jackson Laboratory and backcrossed them one generation into C57Bl/6. We established the lines of mice segregating *Nf1*$^{+/-}$;*p53*$^{+/-}$;Egfr^{wa2}/+, *Nf1*$^{+/-}$;*p53*$^{+/-}$;+/+, *Nf1*$^{+/-}$;*p53*$^{+/-}$;Egfr^{wa-2}/+, and *Nf1*$^{+/-}$;*p53*$^{+/-}$;+/+ by crossing *Nf1*$^{+/-}$;*p53*$^{+/-}$ with Egfr^{wa2}/+ carriers. Mice were housed in a temperature- and humidity-controlled viaticum that was kept on a 12 hr dark/light cycle with free access to food and water. The animal care and use committees of the University of Cincinnati and the Cincinnati Children's Hospital Research Foundation approved all animal use. We genotyped *Nf*1 and p53 alleles as reported (Vogel et al., 1999). We genotyped Egfr^{wa-2} by PCR amplifying a 170 bp region (primers: 5′-CCCAGAAAGGGATATGCG-3′ and 5′-GCAACCGTAGGGCATGAG-3′) and digesting with FokI to produce an uncut 170 bp or cut 75 and 95 bp fragments diagnostic for wild-type (wt) Egfr and Egfr^{wa2} alleles, respectively (Luetteke et al., 1994).

Acknowledgments

We thank Doug Lowy (NCI) for reviewing the manuscript, Charles Kuntz (University of Cincinnati) for helpful discussion, Frank Sharp (University of Cincinnati) for use of the ABI7700 Sequence Detector, Brian Weiss for assistance with statistics, and the University of Cincinnati Transgenic Core for generation of CNPase-hEGFR mice. We thank Maureen Fitzgerald for electron microscopy. This work was supported by grants NIH NS28840 and the DAMD-17-02-1-0679 to N.R. J.W. is a DAMD Neurofibromatosis Fellow. B.C.L. was supported by a fellowship from the Ohio ACS. A NMSS Advanced postdoctoral fellowship and the DOD support S.J.M. K.R.M. was supported by T32-CA-59268 and the Albert J. Ryan Foundation.

Received: January 20, 2003
Revised: October 8, 2004
Accepted: October 25, 2004
Published: January 17, 2005

References

Badache, A., Muja, N., and De Vries, G. (1998). Expression of Kit in neurofibromin-deficient human Schwann cells: Role in Schwann cell hyperplasia associated with type 1 neurofibromatosis. Oncogene *17*, 795–800.

Brannan, C., Perkins, A., Vogel, K., Ratner, N., Nordlund, M., Reid, S., Buchberg, A., Jenkins, N., Parada, L., and Copeland, N. (1994). Targeted disruption of the neurofibromatosis type-1 gene leads to developmental abnormalities in heart and various neural crest-derived tissues. Genes Dev. *8*, 1019–1029.

Brown, M., and Asbury, A. (1981). Schwann cell proliferation in the postnatal mouse: Timing and topography. Exp. Neurol. *74*, 170–186.

Buzard, G., Enomoto, T., Anderson, L., Perantoni, A., Devor, D., and Rice, J. (1999). Activation of neu by missense point mutation in the transmembrane domain in schwannomas induced in C3H/HeNCr mice by transplacental exposure to N-nitrosoethylurea. J. Cancer Res. Clin. Oncol. *125*, 653–659.

Chandross, K., Cohen, R., Paras, P.J., Gravel, M., Braun, P., and Hudson, L. (1999). Identification and characterization of early glial progenitors using a transgenic selection strategy. J. Neurosci. *19*, 759–774.

Chen, S., Rio, C., Ji, R., Dikkes, P., Coggeshall, R., Woolf, C., and Corfas, G. (2003). Disruption of ErbB receptor signaling in adult non-myelinating Schwann cells causes progressive sensory loss. Nat. Neurosci. *6*, 1186–1193.

Cichowski, K., Shih, T.S., Schmitt, E., Santiago, S., Reilly, K., McLaughlin, M.E., Bronson, R.T., and Jacks, T. (1999). Mouse models of tumor development in neurofibromatosis type 1. Science *286*, 2172–2176.

Cunningham, D., Humblet, Y., Siena, S., Khayat, D., Bleiberg, H., Santoro, A., Bets, D., Mueser, M., Harstrick, A., Verslype, C., et al. (2004). Cetuximab monotherapy and cetuximab plus irinotecan in irinotecan-refractory metastatic colorectal cancer. N. Engl. J. Med. *351*, 337–345.

DeClue, J.E., Heffelfinger, S., Benvenuto, G., Ling, B., Li, S., Rui, W., Vass, W.C., Viskochil, D., and Ratner, N. (2000). Epidermal growth factor receptor expression in neurofibromatosis type-1 related tumors and NF1 animal models. J. Clin. Invest. *105*, 1–10.

Evans, D., Baser, M., McGaughran, J., Sharif, S., Howard, E., and Moran, A. (2002). Malignant peripheral nerve sheath tumours in neurofibromatosis 1. J. Med. Genet. *39*, 311–314.

Feldkamp, M., Angelov, L., and Guha, A. (1999). Neurofibromatosis type 1 peripheral nerve tumors: Aberrant activation of the Ras pathway. Surg. Neurol. *51*, 211–218.

Friedman, J., and Birch, P. (1997). Type 1 neurofibromatosis: A descriptive analysis of the disorder in 1,728 patients. Am. J. Med. Genet. *70*, 138–143.

Garratt, A., Britsch, S., and Birchmeier, C. (2000). Neuregulin, a factor with many functions in the life of a schwann cell. Bioessays *22*, 987–996.

Gitler, A., Zhu, Y., Ismat, F., Lu, M., Yamauchi, Y., Parada, L., and Epstein, J.A. (2003). Nf1 has an essential role in endothelial cells. Nat. Genet. *33*, 75–79.

Gravel, M., Di Polo, A., Valera, P., and Braun, P. (1998). Four-kilobase sequence of the mouse CNP gene directs spatial and temporal expression of lacZ in transgenic mice. J. Neurosci. Res. *53*, 393–404.

Grinspan, J., Marchionni, M., Reeves, M., Coulaloglou, M., and Scherer, S. (1996). Axonal interactions regulate Schwann cell apoptosis in developing peripheral nerve: Neuregulin receptors and the role of neuregulins. J. Neurosci. *16*, 6107–6118.

Haney, C., Sahenk, Z., Li, C., Lemmon, V., Roder, J., and Trapp, B. (1999). Heterophilic binding of L1 on unmyelinated sensory axons mediates Schwann cell adhesion and is required for axonal survival. J. Cell Biol. *146*, 1173–1184.

Huijbregts, R., Roth, K., Schmidt, R., and Carroll, S. (2003). Hypertrophic neuropathies and malignant peripheral nerve sheath tumors in transgenic mice overexpressing glial growth factor beta3 in myelinating Schwann cells. J. Neurosci. *23*, 7269–7280.

Huson, S. (1998). Neurofibromatosis type 1: Historical perspective and introductory overview. In Neurofibromatosis Type 1: From Genotype to Phenotype, M. Upadhyaya and D.N. Cooper, eds. (Oxford: BIOS Sci. Pub. Ltd.), pp. 1–13.

Jacks, T., Shih, T.S., Schmitt, E.M., Bronson, R.T., Bernards, A., and Weinberg, R.A. (1994). Tumor predisposition in mice heterozygous for a targeted mutation in NF1. Nat. Genet. *7*, 353–361.

Jessen, K., Morgan, L., Stewart, H., and Mirsky, R. (1990). Three markers of adult non-myelin-forming Schwann cells, 217c(Ran-1), A5E3 and GFAP: Development and regulation by neuron-Schwann cell interactions. Development *109*, 91–103.

Johnson, M., Kamso-Pratt, J., Federspiel, C., and Whetsell, W.J. (1990). Mast cell and lymphoreticular infiltrates in neurofibromas. Comparison with nerve sheath tumors. Arch. Pathol. Lab. Med. *113*, 1263–1270.

Kim, H.A., Rosenbaum, T., Marchionni, M.A., Ratner, N., and DeClue, J.E. (1995). Schwann cells from neurofibromin deficient mice exhibit activation of $p21^{ras}$, inhibition of cell proliferation and morphological changes. Oncogene *11*, 325–335.

Kourea, H., Cordon-Cardo, C., Dudas, M., Leung, D., and Woodruff, J. (1999). Expression of p27(kip) and other cell cycle regulators in malignant peripheral nerve sheath tumors and neurofibromas: The emerging role of p27(kip) in malignant transformation of neurofibromas. Am. J. Pathol. *155*, 1885–1891.

Krishnaswamy, G., Kelley, J., Johnson, D., Youngberg, G., Stone, W., Huang, S., Bieber, J., and Chi, D. (2001). The human mast cell: Functions in physiology and disease. Front. Biosci. *6*, D1109–D1127.

Legius, E., Marchuk, D., Collins, F., and Glover, T. (1993). Somatic deletion of the neurofibromatosis type 1 gene in a neurofibrosarcoma supports a tumor suppressor gene hypothesis. Nat. Genet. *3*, 122–126.

Levi, A., Bunge, R., Lofgren, J., Meima, L., Hefti, F., Nikolics, K., and Sliwkowski, M. (1995). The influence of heregulins on human Schwann cell proliferation. J. Neurosci. *15*, 1329–1340.

Li, H., Velasco-Miguel, S., Vass, W., Parada, L., and DeClue, J. (2002). Epidermal growth factor receptor signaling pathways are associated with tumorigenesis in the Nf1:p53 mouse tumor model. Cancer Res. *62*, 4507–4513.

Luetteke, N.C., Phillips, H.K., Qiu, T.H., Copeland, N.G., Earp, H.S., Jenkins, N.A., and Lee, D.C. (1994). The mouse waved-2 phenotype results from a point mutation in the EGF receptor tyrosine kinase. Genes Dev. *8*, 399–413.

Mata, M., Alessi, D., and Fink, D. (1990). S100 is preferentially distributed in myelin-forming Schwann cells. J. Neurocytol. *19*, 432–442.

Miller, S.J., Li, H., Rizvi, T.A., Huang, Y., Johansson, G., Bowersock, J., Sidani, A., Vitullo, J., Vogel, K., Parysek, L.M., et al. (2003). Brain lipid binding protein in axon-Schwann cell interactions and peripheral nerve tumorigenesis. Mol. Cell. Biol. *23*, 2213–2224.

Morrissey, T., Levi, A., Nuijens, A., Sliwkowski, M., and Bunge, R. (1995). Axon-induced mitogenesis of human Schwann cells involves heregulin and p185erbB2. Proc. Natl. Acad. Sci. USA *92*, 1431–1435.

Murali, R., Brennan, P., Kieber-Emmons, T., and Greene, M. (1996). Structural analysis of p185c-neu and epidermal growth factor receptor tyrosine kinases: Oligomerization of kinase domains. Proc. Natl. Acad. Sci. USA *93*, 6252–6257.

Noble, M.E., Endicott, J.A., and Johnson, L.N. (2004). Protein kinase inhibitors: Insights into drug design from structure. Science *303*, 1800–1805.

Perry, A., Kunz, S., Fuller, C., Banerjee, R., Marley, E., Liapis, H., Watson, M., and Gutmann, D.H. (2002). Differential NF1, p16, and EGFR patterns by interphase cytogenetics (FISH) in malignant peripheral nerve sheath tumor (MPNST) and morphologically similar spindle cell neoplasms. J. Neuropathol. Exp. Neurol. *61*, 702–709.

Prenzel, N., Fischer, O., Streit, S., Hart, S., and Ullrich, A. (2001). The epidermal growth factor receptor family as a central element for cellular signal transduction and diversification. Endocr. Relat. Cancer *8*, 11–31.

Ranson, M., Hammond, L., Ferry, D., Kris, M., Tullo, A., Murray, P., Miller, V., Averbuch, S., Ochs, J., Morris, C., et al. (2002). ZD1839, a selective oral epidermal growth factor receptor-tyrosine kinase inhibitor, is well tolerated and active in patients with solid, malignant tumors: Results of a phase I trial. J. Clin. Oncol. *20*, 2240–2250.

Reilly, K.M., Loisel, D.A., Bronson, R.T., McLaughlin, M.E., and Jacks, T. (2000). Nf1;Trp53 mutant mice develop glioblastoma with evidence of strain-specific effects. Nat. Genet. *26*, 109–113.

Riccardi, V. (1992). Neurofibromatosis: Phenotype, Natural History and Pathogenesis, 2nd edition. (Baltimore, MD: John Hopkins University Press).

Roberts, R.B., Min, L., Washington, M.K., Olsen, S.J., Settle, S.H., Coffey, R.J., and Threadgill, D.W. (2002). Importance of epidermal growth factor

receptor signaling in establishment of adenomas and maintenance of carcinomas during intestinal tumorigenesis. Proc. Natl. Acad. Sci. USA *99*, 1521–1526.

Sawada, S., Florell, S., Purandare, S.M., Ota, M., Stephens, K., and Viskochil, D. (1996). Identification of NF1 mutations in both alleles of a dermal neurofibroma. Nat. Genet. *14*, 110–112.

Serra, E., Puig, S., Otero, D., Gaona, A., Kruyer, H., Ars, E., Estivill, X., and Lazaro, C. (1997). Confirmation of a double-hit model for the NF1 gene in benign neurofibromas. Am. J. Hum. Genet. *61*, 512–519.

Sheela, S., Riccardi, V., and Ratner, N. (1990). Angiogenic and invasive properties of neurofibroma Schwann cells. J. Cell Biol. *111*, 645–653.

Sherman, L., Atit, R., Rosenbaum, T., Cox, A., and Ratner, N. (2000). Singel cell Ras-GTP analysis reveals altered Ras activity in a subpopulation of neurofibroma Schwann cells but not fibroblasts. J. Biol. Chem. *275*, 30740–30745.

Sibilia, M., Fleischmann, A., Behrens, A., Stingl, L., Carroll, J., Watt, F.M., Schlessinger, J., and Wagner, E.F. (2000). The EGF receptor provides an essential survival signal for SOS-dependent skin tumor development. Cell *102*, 211–220.

Stemmer-Rachamimov, A.O., Louis, D.N., Nielsen, G.P., Antonescu, C.R., Borowsky, A.D., Bronson, R.T., Burns, D.K., Cervera, P., McLaughlin, M.E., Reifenberger, G., et al. (2004). Comparative pathology of nerve sheath tumors in mouse models and humans. Cancer Res. *64*, 3718–3724.

Tsukada, Y., and Kurihara, T. (1992). 2′, 3′-cyclic nucleotide 3′-phosphodiesterase: Molecular Characterization and Possible Functional Significance. In Myelin: Biology and Chemistry, R.E. Martenson, ed. (Boca Raton, FL: CRC Press), pp. 449–480.

Velu, T., Beguinot, L., Vass, W., Willingham, M., Merlino, G., Pastan, I., and Lowy, D. (1987). Epidermal-growth-factor-dependent transformation by a human EGF receptor proto-oncogene. Science *238*, 1408–1410.

Vogel, K.S., Klesse, L.J., Velasco-Miguel, S., Meyers, K., Rushing, E.J., and Parada, L.F. (1999). Mouse tumor model for neurofibromatosis type 1. Science *286*, 2176–2179.

Wallace, M., Andersen, L., Saulino, A., Gregory, P., Glover, T., and Collins, F. (1991). A de novo Alu insertion results in neurofibromatosis type 1. Nature *353*, 864–866.

Wechsler, W., Rice, J., and Vesselinovitch, S. (1979). Transplacental and neonatal induction of neurogenic tumors in mice: Comparison with related species and with human pediatric neoplasms. Natl. Cancer Inst. Monogr. *51*, 219–226.

Weissbarth, S., Maker, H., Raes, I., Brannan, T., Lapin, E., and Lehrer, G. (1981). The activity of 2′,3′-cyclic nucleotide 3′-phosphodiesterase in rat tissues. J. Neurochem. *37*, 677–680.

Xu, G., O'Connell, P., Viskochil, D., Cawthon, R., Robertson, M., Culver, M., Dunn, D., Stevens, J., Gesteland, R., White, R., et al. (1990). The neurofibromatosis type 1 gene encodes a protein related to GAP. Cell *62*, 599–608.

Yang, F., Ingram, D., Chen, S., Hingtgen, C., Ratner, N., Monk, K., Clegg, T., White, H., Mead, L., Wenning, M., et al. (2003). Neurofibromin-deficient Schwann cells secrete a potent migratory stimulus for Nf1+/− mast cells. J. Clin. Invest. *112*, 1851–1861.

Yarden, Y. (2001). The EGFR family and its ligands in human cancer. Signalling mechanisms and therapeutic opportunities. Eur. J. Cancer *37*, S3–S8.

Zhu, Y., Ghosh, P., Charnay, P., Burns, D., and Parada, L. (2002). Neurofibromas in NF1: Schwann cell origin and role of tumor environment. Science *296*, 920–922.